

System Level Evaluation of LTE-V2V Mode 4 Communications and its Distributed Scheduling

Rafael Molina-Masegosa and Javier Gozalvez

Universidad Miguel Hernandez de Elche (UMH)
UWICORE laboratory, <http://www.uwicare.umh.es>
Avda. de la Universidad, s/n, 03202, Elche, Spain
rafael.molinam@umh.es, j.gozalvez@umh.es

Abstract— The 3GPP has recently published the first version of the Release 14 standard that includes support for V2V communications using LTE sidelink communications (referred to as LTE-V, LTE-V2X, LTE-V2V or Cellular V2X). The standard includes a mode (mode 4) where vehicles autonomously select and manage the radio resources without any cellular infrastructure support. This is highly relevant since V2V safety applications cannot depend on the availability of infrastructure-based cellular coverage, and transforms LTE-V into a possible (or complimentary) alternative to 802.11p. The performance of LTE-V2V in mode 4 is highly dependent on its distributed scheduling protocol (sensing-based Semi-Persistent Scheduling) that is used by vehicles to reserve resources for their transmissions. This paper presents the first evaluation of the performance and operation of this protocol under realistic traffic conditions in urban scenarios. The evaluation demonstrates that further enhancements should be investigated to reduce packet collisions.

Keywords— *LTE-V, LTE-V2X, LTE-V2V, Cellular V2X, V2V, Vehicle to Vehicle, resource management, distributed scheduling, sensing-based Semi-Persistent Scheduling, 5G, D2D, vehicular networks, cooperative ITS, C-ITS.*

I. INTRODUCTION

Connected vehicles will rely on V2V (Vehicle-to-Vehicle) communications to deploy active safety services. V2V communications are generally characterized by the transmission of small packets (referred to as beacons or CAM messages) with strict latency and reliability requirements. Important research efforts have been devoted over the last years to develop V2V communications using the IEEE802.11p/WAVE and ITS G5 standards. Some studies (e.g. [1]) have highlighted the difficulty of the 802.11p medium access to guarantee QoS levels and ensure the networks' scalability. As an alternative to 802.11p, the Third Generation Partnership Project (3GPP) published in September 2016 the first version of the Release 14 [2] standard that includes support for V2V communications using LTE sidelink communications (commonly referred to as LTE-V, LTE-V2X, LTE-V2V or Cellular V2X). Certain reports claim that LTE-V improves the link budget compared to 802.11p [3]. Modifications to this first version were published in December 2016 [4].

LTE sidelink was introduced for public safety D2D (Device to Device) communications in Release 12. Release 14 introduces two new modes (mode 3 and mode 4) specifically designed for V2V communications [4,5]. In mode 3, two vehicles directly communicate with each other, but the selection and management of the resources is done by the

cellular infrastructure. In mode 4, vehicles autonomously select and manage the resources without any cellular infrastructure support. Mode 4 is highly relevant for vehicular networks as V2V safety applications cannot depend on the availability of infrastructure-based cellular coverage. Release 14 introduces important changes for mode 3 and mode 4 with respect to modes 1 and 2 in Release 12. Modes 1 and 2 were designed with the objective to prolong the battery lifetime through energy-efficient LTE sidelink (D2D) protocols. On the other hand, modes 3 and 4 have been designed with the objective to satisfy the V2V communications requirements in terms of high reliability, low latency and network scalability. To this aim, Release 14 modifies the organization and management of radio resources. In particular, it eliminates the time division of resources into SA (Scheduling Assignment) and Data periods, and organizes resources (RBs, Resource Blocks) into frequency sub-channels. Vehicles can now reserve a resource and transmit a packet at any point in time. This can reduce the latency at the expense of the energy-efficiency since vehicles need to be permanently in reception mode (i.e. discontinuous reception is not anymore possible in modes 3 and 4). Another important novelty introduced in mode 4 is the distributed scheduling protocol used by vehicles to autonomously select their radio resources when they cannot rely on the assistance of the cellular infrastructure¹. The protocol is referred to as sensing-based Semi-Persistent Scheduling (SPS). Its objective is to improve the reliability of V2V communications without overloading the channel with retransmissions. To this aim, it exploits the periodic nature of beacons or CAM packets, and introduces a semi-persistent reservation of resources. Vehicles can then sense the previous transmissions to estimate which resources are free and avoid packet collisions. The capacity for LTE sidelink mode 4 to guarantee reliable V2V communications strongly depends on the adequate operation of the sensing-based SPS scheme. To date, the only studies available that have analyzed its performance are those presented at the 3GPP working groups (e.g. [6])². These studies generally focus only on Packet Delivery Ratio (PDR) performance, and they consider simple mobility models that do not reflect realistic traffic patterns. These patterns can have a significant impact on e.g. packet collisions or scalability evaluations. This study extends the current state of the art by presenting what is to the authors' knowledge, the first analysis

¹ D2D nodes randomly select the radio resources in mode 2 of Release 12. Up to four retransmissions per packet are allowed to increase reliability.

² [7] presents an analysis of V2V communications using an earlier version of LTE sidelink that does not correspond to that presented under Release 14.

of the performance and operation of V2V communications using the 3GPP LTE sidelink mode 4 under realistic mobility patterns in a urban scenario. In addition, this paper analyses the operation of the sensing-based SPS resource allocation process, and quantifies the type of transmission errors encountered in order to identify areas where further improvements should be investigated.

II. LTE-V2V MODE 4 COMMUNICATIONS

A. Frame structure and Resource Pool Framework

This study considers the scenario where 10MHz of spectrum is exclusively reserved for V2V communications³. Modes 3 and 4 divide the channel bandwidth in sub-channels. The number of RBs (of 180kHz) per sub-channel can vary. A Transport Block (TB) contains a full beacon or CAM packet. A node that wants to transmit a TB must also transmit an associated Sidelink Control Information (SCI)⁴ message that other nodes must correctly receive to be able to decode the transmitted TB. The first two RBs of each sub-channel (Pool SCI+Data in Fig. 1) can be used to transmit an SCI or part of a TB. The rest of RBs of a sub-channel can only be used to transmit the TB (Pool Data Only in Fig. 1). The SCI must always be transmitted in the same sub-frame as the associated TB, and occupies the first 2 RBs of the first utilized sub-channel. The TB is transmitted in the RBs following the SCI, and can occupy RBs of the other sub-channels depending on the size of the TB. The standard considers the option that the SCI and associated TB do not occupy adjacent RBs. However, the TB cannot be divided, and adjacent RBs must always be used for its transmission. The transmission of an SCI and its associated TB in the same sub-frame is referred to as SCI+TB in this paper.

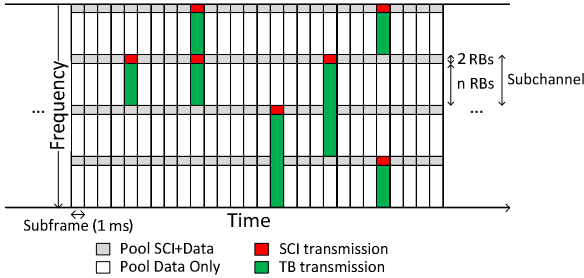


Fig. 1. Frame structure and example of the utilization of resources.

B. Sensing-based Semi-Persistent Scheduling

Vehicles can reserve sub-channels to transmit several consecutive packets using the sensing-based SPS scheme that is here described [5,8]. Packets can be transmitted every 100 sub-frames (i.e. 10 packets per second) or in multiples of 100 sub-frames (up to a minimum of 1 packet per second). The packet transmission interval is indicated in the SCI so that other vehicles can estimate which sub-channels could be free. Let's suppose that a vehicle V needs to reserve new sub-channels at time T in order to transmit a packet. It can reserve

sub-channels between T and the established maximum latency (equal or lower than 100ms [5]). This time period is referred to as selection window. Within the selection window, a candidate resource to be reserved is defined as a group of adjacent sub-channels within the same sub-frame where the SCI+TB to be transmitted fits. The vehicle analyzes all Candidate Resources (CR) in the selection window, and excludes those for which:

- It has correctly received in the last 1000 subframes an SCI from another vehicle indicating that it will utilize such resource at the same time as it would need it to transmit one of its packets;
- And the RBs utilized to transmit the TB associated to the received SCI (previous condition) experience an average Reference Signal Received Power (RSRP) higher than a given threshold⁵. The number of non-excluded candidate resources must be equal or higher than 20% of all candidate resources in the selection window. If not, this second condition is executed iteratively with a 3dB higher RSRP threshold at each iteration until the 20% target is met.

Vehicle V creates then a list of non-excluded candidate resources. The total number of candidate resources in the list must be equal to 20% of the candidate resources in the selection window. The list is composed of the candidate resources that experienced the lowest average RSSI (Received Signal Strength Indicator) over all its RBs in all the previous $T_{CR}-100*j$ sub-frames (Fig. 2); j is an integer variable that takes the values from 1 to 10. Vehicle V randomly chooses one of the candidate resources in the list, and reserves it for the next *Resource Counter* packet transmissions. This counter is randomly set between 5 and 15. After each packet transmission, the *Resource Counter* is decremented by one, and when it is equal to zero⁶, new resources must be selected again with probability $(1 - P)$. P can be set between 0 and 0.8. Even if the same resources are maintained when *Resource Counter* reaches zero, the value of *Resource Counter* must be again randomly chosen between 5 and 15.

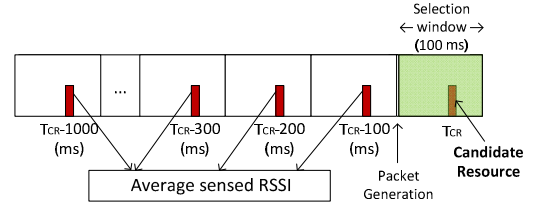


Fig. 2. Estimation of average RSSI of a candidate resource

The reliability of V2V communications can be increased in LTE sidelink mode 4 by retransmitting each packet once⁷. The sensing-based SPS scheme creates a second list of candidate resources for the redundant SCI+TB transmission. Let's suppose that the original SCI+TB transmission took place in a candidate resource in sub-frame SF . This second list is made of all candidate resources in the selection window that are located in the time interval $[SF-15ms; SF+15ms]$, except for all the

³ The 3GPP standards also consider the option where a given channel can be shared in overlay mode between V2V and other type (e.g. cellular) of communications.

⁴ Also referred to as SA Scheduling Assignment in 3GPP working groups.

⁵ If V receives several SCIs from the same interfering vehicle reserving a given CR, it will utilize the most recent one to estimate the average RSRP.

⁶ New resources need to be reserved also if the packet to be transmitted at a given point in time does not fit in the sub-channels previously reserved.

⁷ Referred in 3GPP standards as HARQ retransmission.

candidate resources in *SF*. The sensing-based SPS scheme randomly selects a resource from this second list for the redundant SCI+TB transmission.

III. SIMULATION ENVIRONMENT

This study evaluates the performance and operation of LTE sidelink mode 4 for V2V communications using the Veins simulation platform. Veins integrates OMNET++ for wireless networking simulation with the open-source traffic simulation platform SUMO. We have implemented in Veins a new interface for LTE sidelink mode 4.

The evaluation has been done under the Urban Case scenario defined in [9] and that is generally utilized by the 3GPP working groups. The scenario models a Manhattan grid layout of 9 by 7 building blocks. Each block has a size of 250m by 433m. Each street has 2 lanes in each direction, and the width of each lane is equal to 3.5m. Each street has a 3m sidewalk on each side. To avoid border effects, the results presented in this paper correspond to those obtained on a single street between the four central intersections of the scenario. Random vehicular routes are generated using SUMO, and the average traffic density has been set to 85 vehicles per kilometer following the indications in [9] for the urban scenario. In [9], vehicles are initially positioned in the scenario using a spatial Poisson distribution, and they move at a constant speed of 60 km/h. This modelling does not reflect realistic traffic patterns as vehicles overrun each other, and it does not take into account, for example, the traditional stop and go at intersections. This simple modelling can have important implications in the evaluation of LTE-V2V as it will not be able to adequately capture the potential packet collisions that could be generated at intersections where higher densities of vehicles generally concentrate. Using SUMO, our simulations consider realistic traffic patterns as the mobility of vehicles is implemented using the Krauss car following model. Vehicles have then a variable speed based on their location and surrounding traffic context. The maximum speed has been set to 15 km/h in order to achieve the density of 85 vehicles per km considered in [9].

The propagation is modeled using the WINNER+ B1 pathloss model for Manhattan layouts. The shadowing is modeled with a log-normal distribution with 3dB standard deviation under LOS (Line of Sight) conditions and 4dB under NLOS (Non Line of Sight). We have implemented the shadowing spatial correlation as in [9] with a decorrelation distance of 10m. The pathloss and shadowing are used to estimate the SINR (Signal to Interference Noise Ratio) for each received packet. The estimated SINR is used together with the BLER (Block Error Rate)-SINR curves presented in [10] to estimate the BLER for each received packet. This BLER value is used together with a random number to decide whether the packet is correctly decoded or not. Our simulations consider a single 10MHz channel at 5.9GHz that is exclusively reserved for V2V communications. We assume perfect synchronization and all vehicles transmit at 23dBm. The noise figure is set to 9dB and In-Band Emissions (IBE) are modeled as in [9].

Packets are generated following the model described in [9] that provides a simplified representation of the CAM and BSM packets transmitted in vehicular networks [11]. The model

generates packets with a period of 100ms. One out of every five packets has a size of 300 bytes, while the other packets have a size of 190 bytes. The 300 bytes packets are coded with a MCS (Modulation and Coding Scheme) using QPSK and a $\frac{1}{2}$ code rate (TBs occupy 20 RBs). The 190 bytes packets are coded with a MCS using QPSK and a 0.7 code rate (TBs occupy 10 RBs). The 3GPP Release 14 standards do not specify the value for certain parameters: number of RBs per sub-channel, maximum permitted latency, RSRP threshold, and *P*. This study considers sub-channels of 12 RBs (2 RBs for SCI or TB, and 10 RBs only for TB). The 10MHz channel (with 50 RBs of 180kHz per sub-frame) can then accommodate 4 sub-channels. The transmission of 190-bytes packets completely occupy a sub-channel. The 300-bytes packets occupy the first 22 RBs of two adjacent sub-channels in the same sub-frame. The maximum latency has been set to 100ms, and the selection window is equal to 100 sub-frames. The average RSRP threshold has been set to -110dBm. *P* has been set equal to 0.

IV. RESULTS

Sufficient simulations have been conducted to guarantee a relative error below 5% for all results presented in this section. Fig. 3 illustrates the Packet Delivery Ratio (PDR) obtained with V2V communications using LTE sidelink mode 4. The PDR is represented as a function of the distance between transmitter and receiver. Fig. 3 corresponds to the PDR for all transmissions in the scenario, while Fig. 4 and Fig. 5 represent it only for V2V transmissions under LOS and NLOS conditions respectively. All three figures depict the PDR achieved when utilizing the sensing-based SPS scheme to select resources (*Sensing*) and when such resources are randomly selected (*Random*). The PDR is shown when each packet is transmitted using one SCI+TB transmission or two (for redundancy). The depicted results show that the sensing-based SPS scheme improves the performance over a random selection of resources for short and medium distances, and in particular under LOS conditions. The difference between the sensing-based SPS scheme and a random selection of resources decreases with the distance. In addition, it is important noting that the gains achieved with the sensing-based SPS scheme are higher when each packet is transmitted only once. When redundancy is added, the PDR improves, but there is little difference in urban scenarios between assigning radio resources randomly or using the sensing-based SPS scheme included in the 3GPP Release 14 standard.

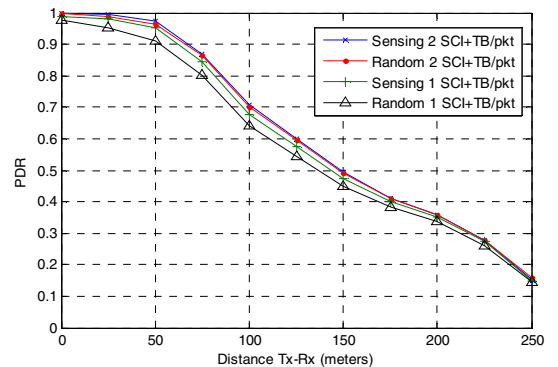


Fig. 3. PDR as a function of the distance between transmitter and receiver.

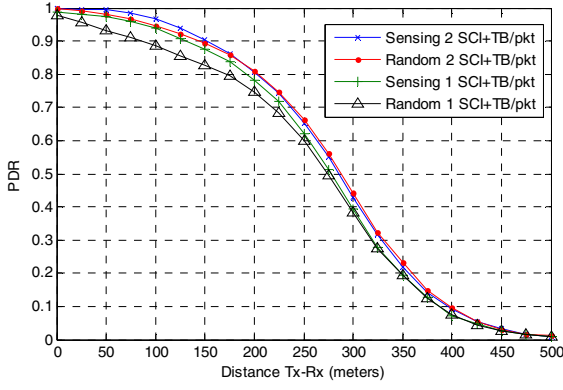


Fig. 4. PDR as a function of the distance between transmitter and receiver under LOS conditions.

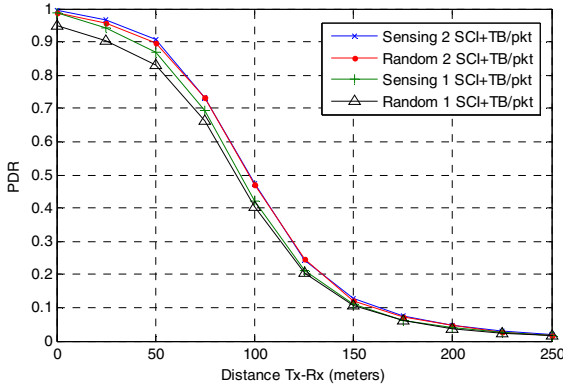


Fig. 5. PDR as a function of the distance between transmitter and receiver under NLOS conditions.

To understand the results and trends depicted in Figs. 3 to 5, it is necessary to analyze the operation of the sensing-based SPS scheme. To this aim, we have analyzed the different type of transmission errors that can occur. Such errors are analyzed per single SCI+TB transmission of each packet, and we focus on the TB transmission errors that can be classified as:

1) *Half-Duplex*. A TB cannot be received because the receiver was transmitting in the same sub-frame.

2) *Propagation*. The reception of the TB fails because it has not been received with sufficient SNR to correctly decode it. This type of error excludes those quantified in 1), and does not consider interference/collisions.

3) *Collision*. The reception of a TB fails because it has not been received with sufficient SINR to correctly decode it as a result of the interference/collisions from other vehicles. This type of error excludes those quantified in 1) and 2).

4) *No SCI*. To correctly receive a TB, it is necessary to also correctly receive the associated SCI. This error quantifies the occasions in which the transmission of a TB did not experience any of the errors quantified in 1), 2) and 3), but the TB cannot be correctly received because the reception of the associated SCI failed.

A TB is then correctly received when none of the four type of errors occur. To calculate the relevance of each transmission error, we denote as N_{total} the total number of transmitted TBs.

N_{error} denotes the total number of transmitted TBs that have not been correctly received. N_{sensed} represents the number of TBs that have been received with sufficient SNR, and hence do not experience Half-Duplex or propagation errors. N_{sensed} includes the TBs correctly received and those that fail due to collisions or because the associated SCI is not correctly received. The variables and types of errors are represented in Fig. 6.

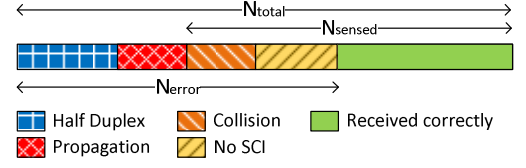


Fig. 6. Types of TB transmission errors.

Fig. 7 represents the percentage of TBs incorrectly received per type of transmission error as a function of the distance between transmitter and receiver. The depicted percentage values are computed with respect to N_{total} , and hence provide an indication of the relevance of each type of error in absolute terms. Fig. 8 also represents the percentage of TBs incorrectly received per type of transmission error, but in this case the percentage values are computed with respect to N_{error} . Fig. 8 hence provides an indication of the relative relevance of each type of error as a function of the distance (the sum of percentage errors for a given distance in Fig. 8 is equal to 100%). Finally, Fig. 9 depicts the percentage of TBs incorrectly received due to collisions (again estimated with respect to N_{sensed}). This metric has been estimated to analyze the relevance of packet collisions, and hence provide valuable information about whether the sensing-based SPS scheme is adequately managing the resources. Figs. 7 to 9 correspond to the performance achieved with the sensing-based SPS scheme defined in LTE sidelink mode 4 for V2V communications under LOS. Similar trends have been observed for NLOS, although the effects are experienced at shorted distances.

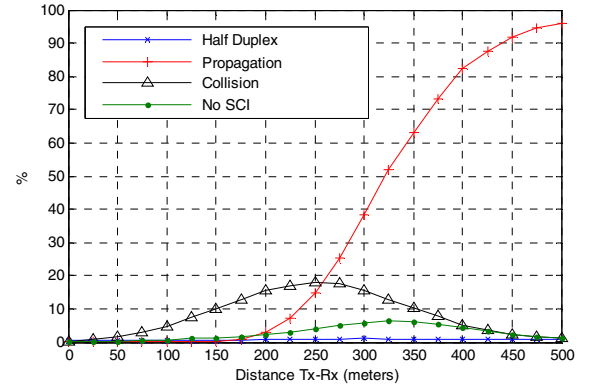


Fig. 7. Percentage of TBs incorrectly received per type of transmission error as a function of the distance between transmitter and receiver (values estimated with respect to N_{total}). Single SCI+TB transmission per packet.

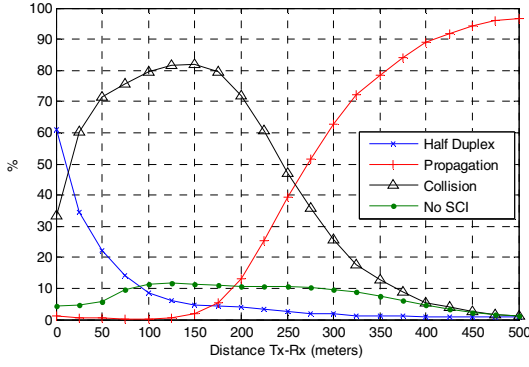


Fig. 8. Percentage of TBs incorrectly received per type of transmission error as a function of the distance between transmitter and receiver (values estimated with respect to N_{error}). Single SCI+TB transmission per packet.

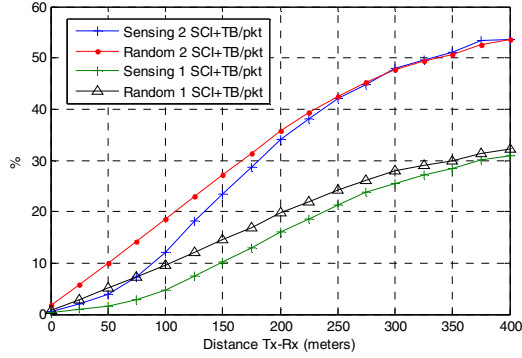


Fig. 9. Percentage of TBs incorrectly received due to collisions as a function of the distance between transmitter and receiver (with respect to N_{sensed}).

Fig. 8 shows that packet collisions are the predominant TB transmission error up to 250m under LOS conditions. From this point onwards, most transmission errors are due to propagation conditions. When looking in absolute terms, Fig. 7 shows that the percentage of TB transmissions that suffer collisions is actually non negligible. For example, at 250m distance, around 20% of all transmitted TBs are incorrectly received due to collisions with other vehicles that share the same resources. These results show that there is a considerable margin of improvement, and further enhancements to the sensing-based SPS scheme should be investigated.

Fig. 9 shows that the TB transmission errors due to packet collisions increase with the distance⁸. The probability that interfering vehicles can produce sufficient interference to provoke a transmission error decreases when transmitter and receiver are at short distances. This probability increases when the distance increases, which explains the trends observed in Fig. 9. This figure also compares the operation of the sensing-based SPS scheme with a random selection of resources per vehicle. It is interesting to observe that the major gains achieved with the sensing-based SPS scheme are obtained at short to medium distances, and when only one transmission is done per packet (i.e. no redundancy is introduced). This trend

is explained by the impact of the hidden terminal problem when the distance between transmitter and receiver increases. The relevance of this problem increases with the channel utilization as observed in Fig. 9. When redundancy is introduced, sensing-based SPS results in the same probability of packet collision as vehicles randomly selecting their resources. This result is due to the process defined in sensing-based SPS to identify the candidate resources. When packet collisions increase, more SCIs are incorrectly received and hence resources that are occupied by interfering vehicles are not excluded from the list of candidate resources explained in Section II.B. This results in more packet collisions, and the gains obtained with the sensing-based SPS scheme are reduced.

V. CONCLUSIONS

This paper has presented the first evaluation of the performance and operation of LTE-V2V mode 4 communications under realistic traffic conditions in urban scenarios. The study has also analyzed and quantified the different type of transmissions errors that the sensing-based SPS protocol can suffer. The conducted evaluation has demonstrated that the protocol can experience significant packet collisions, and its benefits decrease with the distance between transmitter and receiver and the channel load. Further enhancements to the sensing-based SPS protocol, or alternative schemes, should hence be investigated.

REFERENCES

- [1] G. Araniti, C. Campolo, M. Condoluci, A. Iera and A. Molinaro, "LTE for Vehicular Networking: A Survey," IEEE Communications Magazine, Volume: 51, Issue: 5, May. 2013.
- [2] 3GPP TS 36.300, "Evolved Universal Terrestrial Radio Access (E-UTRA) and Evolved Universal Terrestrial Radio Access Network (E-UTRAN); Overall description; Stage 2," Rel-14 V14.0.0, Sep. 2016.
- [3] 5G Americas, "V2X Cellular Solutions", Oct. 2016.
- [4] 3GPP TS 36.300, "Evolved Universal Terrestrial Radio Access (E-UTRA) and Evolved Universal Terrestrial Radio Access Network (E-UTRAN); Overall description; Stage 2," Rel-14 V14.1.0, Dec. 2016.
- [5] 3GPP TS 36.213, "Evolved Universal Terrestrial Radio Access (E-UTRA); Physical layer procedures," Section 14, Rel-14 V14.1.0, Dec. 2016.
- [6] R1-1609955, "Remaining Issues for V2V," Qualcomm Incorporated, 3GPP TSG RAN WG1 Meeting #86b, Lisbon, Portugal, Oct. 2016.
- [7] S. Chen, J. Hu, Y. Shi and L. Zhao, "LTE-V: A TD-LTE based V2X Solution for Future Vehicular Network," IEEE Internet of Things Journal, in press.
- [8] 3GPP TS 36.321, "Evolved Universal Terrestrial Radio Access (E-UTRA); Medium Access Control (MAC) protocol specification," Rel-14 V14.1.0, Dec. 2016.
- [9] 3GPP TR 36.885, "Study on LTE-based V2X Services," Annex A: Evaluation methodology, Rel-14 V14.0.0, Jun. 2016.
- [10] R1-160284, "DMRS enhancement of V2V," Huawei, HiSilicon, 3GPP TSG RAN WG1 Meeting #84, St Julian's, Malta, Feb. 2016.
- [11] R1-153803, "V2V Traffic model and performance metrics," Huawei, HiSilicon, 3GPP TSG RAN WG1 Meeting #82, Beijing, Aug. 2015.

⁸ It is important to remember that the values reported in Fig. 9 are obtained with respect to N_{sensed} , i.e. without consider propagation errors as in Fig. 7. The percentage of collision errors in Fig. 7 decreases with the distance from 250m simply because these results are computed with respect to N_{total} , and as shown in Fig. 8 propagation errors are predominant from this distance.